Foxn1 and Mmp-9 expression in intact skin and during excisional wound repair in young, adult, and old C57Bl/6 mice

Marta M. Kopcewicz, MSc[1]; Anna Kur-Piotrowska, MSc[1]; Joanna Bukowska, PhD[1]; Jeffrey M. Gimble, MD, PhD[2,3]; Barbara Gawronska-Kozak, PhD[1]

1. Institute of Animal Reproduction and Food Research, Polish Academy of Sciences, Olsztyn, Poland,
2. LaCell LLC, New Orleans, Louisiana, USA, and
3. Departments of Medicine, Structural and Cellular Biology, and Surgery and Center for Stem Cell Research and Regenerative Medicine, Tulane University School of Medicine, New Orleans, Louisiana, USA

Reprint requests:
Barbara Gawronska-Kozak, Institute of Animal Reproduction and Food Research, Polish Academy of Sciences, ul. Tuwima 10 10-748, Olsztyn, Poland.
Tel: (4889) 5234634;
Fax: (4889) 5240124;
Email: b.kozak@pan.olsztyn.pl

Manuscript received: June 23, 2016
Revised: December 21, 2016
Accepted in final form: January 31, 2017

DOI:10.1111/wrr.12524

ABSTRACT

The transcription factor Foxn1 is essential for skin development. Our previous studies performed on young C57BL/6J mice model showed that Foxn1 acts as regulator of the skin wound healing process. The present study extended our initial research regarding the expression and potential role of Foxn1 in the intact and wounded skin as a function of animal age and stage of the wound healing process. We analyzed Foxn1 and Mmp-9 expression in the intact and postinjured skin of young, adult, and old C57BL/6J and transgenic Foxn1::Egfp mice. The similar levels of epidermal *Foxn1* mRNA expression were detected in young and adult C57BL/6J mice and higher levels in old animals. Postinjured skin tissues displayed a gradual decrease of *Foxn1* mRNA expression at Days 1, 5, and 7 after injury. Foxn1-eGFP positive cells were abundant at wound margin and in re-epithelialized epidermis at postwounded Days 1, 5, and 7 and colocalized with E-cadherin and Mmp-9. Postwounded skin at Days 14–36 displayed Foxn1-eGFP cells in the epidermis and in the dermal part of the skin (papillary dermis). A subset of Foxn1-eGFP positive cells in the papillary dermis expressed the myofibroblast marker αSMA. Flow cytometric analysis of cells isolated from postwounded (Day 7) skin tissues showed a significant increase in the percentage of Foxn1-eGFP positive cells with phenotype of double positivity for E-cadherin/N-cadherin (epithelial/mesenchymal markers). Collectively, these data identify the transcription factor Foxn1 as a potential key epidermal regulator modifying both epidermal and dermal healing processes after cutaneous wounding.

Cutaneous wound healing in mammals is a highly coordinated physiological process which restores tissue integrity. The process consists of three overlapping stages: inflammation, new tissue formation, and remodeling.[1] Immediately after injury, the components of the coagulation pathways and inflammatory response act to prevent blood loss, remove debris, and prevent infection. In the second stage of wound repair new tissue formation occurs, whereby keratinocytes, dermal fibroblasts, and other cells proliferate and migrate to fill the wound gap and re-establish the skin barrier. During this phase, extracellular matrix is synthesized by interacting fibroblasts and myofibroblasts. In the third and final stage of wound repair, remodeling occurs with reorganization of the immature extracellular matrix, apoptosis of a variety of cell types at the wound site, and the formation of scar tissue which never achieves the strength and functionality of the original uninjured skin.[2,3]

In contrast, the wound healing process in mammals can follow a different pathway of resolution that restores postwounded skin tissues through a process of regeneration/scar-free healing. More than 35 years ago, Rowlatt reported the seminal finding that mammalian fetuses re-establish the integrity of postwounded skin through process of regeneration that does not form a scar.[4] Since then, scar-less wound healing has been reported in the fetuses of mice, rats, sheep, pigs, monkeys, and humans.[5,6] Mammalian fetuses display scar-free healing only during the first two trimesters of gestational development. By the third trimester, cutaneous wounds heal with a scar, the healing pattern characteristic for adult mammals. Comprehensive studies have recognized several factors and pathways participating in regenerative and reparative skin wound healing processes. However, understanding of the molecular mechanisms that redirect the healing pathway from scar-forming to scar-free remains to be determined. Transcription factors, such as PPARs, Smads, and Homeobox, synchronize the events of the skin wound healing process controlling the expression of effector genes including cytokines, growth factors, and proteolytic enzymes (i.e., matrix metalloproteinases [Mmps]).[7,8] However, none of the transcription factors involved in the skin wound healing

process have yet to provide a satisfactory explanation accounting for the different pathways of skin wound healing resolution over the course of an individual's lifetime.

Our attention has been focused on transcription factor Foxn1 which belongs to the forkhead gene family that comprises a diverse group of winged-helix transcription factors. The expression of Foxn1 is limited to epithelial cells of skin and thymus.[9] In the skin, Foxn1 regulates the balance between keratinocytes growth and differentiation in the epidermis and participates in normal hair follicle development. In the interfollicular epidermis, Foxn1 expression is restricted mainly to the first suprabasal layer, which contains cells in the early stages of terminal differentiation.[9] Remarkably the analysis of postwounded skin tissues of Foxn1 deficient (nude) adult mice revealed their ability to undergo a scar-free skin wound healing process in a manner similar to mammalian fetuses.[10,11]

A characteristic of regenerative healing common to both mammalian fetuses and nude mice is the deficiency (nude mice) or inactivity (fetuses) of the transcription factor Foxn1. Moreover, our recent experiments performed on young (28- to 35-day old) mice showed that Foxn1 acts as regulator of the skin wound healing process through engagement in re-epithelization and in the epithelial-mesenchymal transition (EMT) process during the early stage (Days 1–7) of skin wound healing.[12]

The present study performed on young, adult and old mice focused on [1] determining Foxn1 expression in intact skin across the lifespan; [2] estimating changes in Foxn1 expression and localization during skin wound healing process with correlation to animal age; and [3] examining concomitant changes in Mmp-9 expression as a part of the tissue response to injury.

MATERIALS AND METHODS

Animals

The study was performed on young (21–28 days), adult (2–3 months and 9 months), and old (16–18 months) C57BL/6J (B6) wild type and Foxn1::Egfp transgenic mice. In Foxn1::Egfp mice enhanced green fluorescent protein transgene is driven by *Foxn1* regulatory sequence.[13,14] Transgenic mice were used for flow cytometry and immunohisto- and immunofluorescent analyses to determine the percent of Foxn1-eGFP positive cells and the localization of Foxn1 in skin tissues. To eliminate the possible effect of genetic modification caused by eGFP transgene insertion in *Foxn1* promoter region (Foxn1::Egfp mice), wild type B6 mice were used for qRT-PCR analysis.[12] All mice were obtained from colonies established at the animal facility of the Institute of Animal Reproduction and Food Research of Polish Academy of Sciences. B6 mice were originally purchased from The Jackson Laboratory (Bar Harbor, ME). Four Foxn1::Egfp transgenic males were a kind gift from Professor Thomas Boehm (Max-Planck Institute of Immunobiology and Epigenetics, Germany). The Foxn1::Egfp hemizygotes were generated by breeding Foxn1::Egfp males with B6 females. Foxn1::Egfp genotype was confirmed by PCR (forward primer: GTC CCT AAT CCG ATG GCT AGC TC; reverse primer: GTG CAG ATG AAC TTC AGG GTC) (Genomed, Poland). DNA for genotyping assay was extracted from tail-clipped tissues using the proteinase K (Sigma-Aldrich, MO) and standard phenol-chloroform-isoamyl alcohol DNA (Sigma-Aldrich, MO) isolation protocol. PCR reactions were set up with 2 ng of genomic DNA [10 ng/μL].

All experimental animal procedures were approved by the Ethics Committee of the University of Warmia and Mazury, No. 28/2012.

Epidermis and keratinocytes isolation from uninjured skin tissues for qRT-PCR and flow cytometry analyses

Young, adult, and old ($n = 6$ per age group) B6 mice were used for qRT-PCR analysis. New born ($n = 11$), adult ($n = 10$), and old ($n = 6$) Foxn1::Egfp transgenic mice were applied for flow cytometry assay. Mice were sacrificed using CO_2 asphyxiation and shaved with electric shaver. Using forceps and scissors a full length dorsal midline incision from the head to the tail was made. Starting from the dorsal incision, two circumferential incisions (one just behind the forepaws and the other just before the hind paws) were created. Skin was collected in PBS with 1% penicillin/streptomycin (Sigma-Aldrich, MO). Fat and blood vessels covering the dermis were scraped away until the dermis was clearly and uniformly exposed. Skin tissues were incubated overnight in 6 U/mL dispase (Life Technologies, CA) in Hanks' balanced salt solution (HBSS; Sigma-Aldrich, MO) at 4 C. The following day, using scalpel and forceps, the epidermis was separated from the dermis. For qRT-PCR analysis, the epidermis from B6 mice was immediately stored in TRI reagent (Sigma-Aldrich, MO) in −80 C for subsequent RNA isolation. For flow cytometry assay, the epidermis was digested in 0.05% trypsin (Sigma-Aldrich, MO) for 10 minutes. The trypsin was neutralized with culture medium containing DMEM/F12 (Life Technologies, CA), 15% fetal bovine serum (FBS; Life Technologies, CA), and 1% penicillin/streptomycin (Sigma-Aldrich, MO). The resulting cell suspensions were filtered through a series of cell strainers (100, 70, and 40 μm; BD Biosciences, NJ) and then centrifuged at 1,300 rpm for 9 minutes. Pelleted cells were resuspended in 1 mL of PBS (Gibco, MA) with 0.5% FBS. The number and viability of isolated keratinocytes was determined with a Countess (Invitrogen, CA).

Wound model

Young, adult, and old B6 and Foxn1::Egfp mice were used for skin wound healing experiment (Figure 1; The scheme of the experimental design). The day before wounding mice were anesthetized with isoflurane and shaved in the dorsal area. The following day, mice were anesthetized with isoflurane and four full-thickness excisional wounds were created on the back of individual mice using a sterile 4 mm biopsy punch (Miltex, PA). The surgical procedures were designed to minimize the suffering of the experimental animals. After wounding mice were placed in a warmed cage until recovery before being transferred to individual cages where they were housed separately for the duration of the study. Experimental animals were monitored daily for any signs of infection. Mice were sacrificed at Days 1, 5, 7, 14, 21, and 36 after wounding. 8 mm diameter biopsy punches were used to collect postwounded skin area.

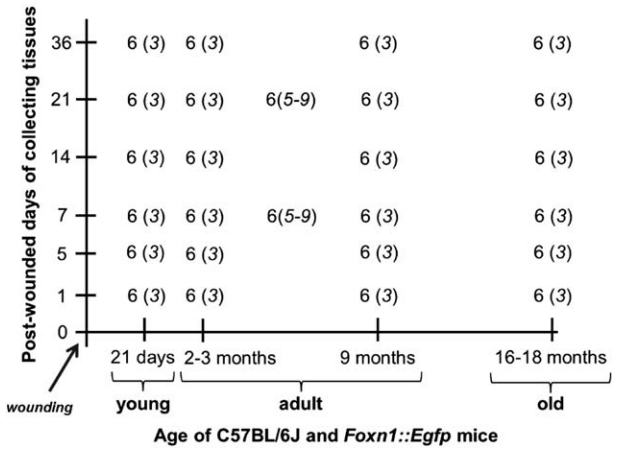

Figure 1. The scheme of experimental design. Young (21-day old), adult (2- to 3- and 9-month old), and old (16- to18-month old) B6 and Foxn1::Egfp mice were injured at Day 0. Skin tissues were collected at Day 0 (uninjured control) and postwounded Days: 1, 5, 7, 14, 21, and 36; $n = 6$ for B6, $n = 3$ for Foxn1::Egfp per time point. At postwounded Days: 7 and 21skin tissues collected from Foxn1::Egfp ($n = 5$–9) and control B6 ($n = 6$) adult mice were used for flow cytometry analyses.

Tissue samples ($n = 6$ per time point) for total RNA isolation and gene expression analysis were immediately frozen in liquid nitrogen and stored at −80 C until further use. Samples for histology were fixed in 10% formalin (Sigma-Aldrich, MO) ($n = 3$–6 per time point) or 4% paraformaldehyde (PFA; Sigma-Aldrich, MO; $n = 3$–6 per time point). Adult Foxn1::Egfp mice at postwounded Days 7 and 21 ($n = 5$–9 per group) and B6 ($n = 6$; control for eGFP specificity signal) were used for flow cytometry assay. Cells were isolated from postwounded total skin samples as previously described.[12]

RNA isolation and quantitative RT-PCR

Total RNA was extracted from skin samples and enzymatically separated epidermis using TRI Reagent (Sigma-Aldrich, MO) according to the manufacturer's instructions. Quantity and quality of RNA was checked on NanoDrop 1000 (Thermoscientific, MA) and agarose gel electrophoresis. cDNA was synthesized from 500 ng of total RNA using High-Capacity cDNA Reverse Transcription Kit with RNase Inhibitor (Applied Biosystem, MA). To measure the levels of *Foxn1*, *Mmp-9*, and *Hprt1* mRNA expression, Single Tube TaqMan® Gene Expression Assays (Life Technologies, CA) were used. Amplification was performed using 7900HT Fast Real-Time PCR System under conditions: initial denaturation for 10 minutes at 95 C, followed by 40 cycles of 15 seconds at 95 C and 1 minute at 60 C. Each run included standard curve based on aliquots of pooled skin RNA. All samples were analyzed in duplicates. After literature review[15] and evaluation of different housekeeping genes: glyceraldehyde 3-phosphate dehydrogenase (*Gapdh*), TATA-binding protein (*Tbp*), and hypoxanthine phosphoribosyl transferase 1 (*Hprt1*) for their expression stability, *Hprt1* was chosen as it was the most stable gene during cutaneous wound healing. mRNA expression levels were normalized to the reference gene *Hprt1* and multiplied by 10.

Immunofluorescence and immunohistochemistry

Skin tissue samples from Foxn1::Egfp mice were fixed for 2 hours in 4% PFA (Sigma-Aldrich, MO), washed twice in PB buffer (pH = 7.4, 0.1 M) and -incubated in PB overnight at +4 C. On the next day, tissue samples were transferred into 18% sucrose in PB with 0.01% sodium azide (Sigma-Aldrich, MO) and stored at +4 C until cryosectioned. Immunofluorescence and immunohistochemistry was performed on 8 μm cryostat sections. For immunofluorescence, the following primary antibodies were used: αSMA (rabbit anti-mouse, Thermoscientific, MA) E-cadherin (rat anti-mouse, Invitrogen, MA), Mmp-9 (rabbit anti-mouse, Millipore, MA). The following secondary antibodies were used: Alexa Fluor 594 goat anti-rabbit IgG (Life Technologies, CA) and Alexa Fluor 594 donkey anti-rat IgG (Life Technologies, CA). Nuclei were counterstained with ProLong® Gold Antifade Mountant with DAPI (Life Technologies, CA). Immunohistochemical staining for the presence of eGFP was performed with anti-eGFP polyclonal antibodies (Abcam, Cambridge, UK). Antibody binding was detected with the ABC complex (Vectastain ABC kit, Vector Laboratories, Inc., CA). In control sections primary antibodies were substituted with non-specific-immunoglobiulin G (IgG). Peroxidase activity was revealed using 3.3′-diaminobenzidine (Sigma-Aldrich, MO) as a substrate. Slides counterstained with hematoxylin were visualized using Olympus microscope (BX43), photographed with Olympus digital camera (XC50) and analyzed with Olympus CellSens Software). Confocal images were scanned and digitalized using an F10i-LIV Laser Scanning Microscope integrated with FLUOVIEW Software (Olympus), with a 60x objective lens. The sequential scans were acquired with Z spacing of 0.5 μm and 1,024 × 1,024 pixel size at room temperature.

Flow cytometry analysis

Keratinocytes from Foxn1::Egfp mice were analyzed for expression of E-cadherin and N-cadherin using flow cytometry based on methods described previously by Gawronska-Kozak et al.[12] Briefly, freshly isolated cells were suspended at a concentration of $0.5 – 1.0 \times 10^6$ cells in warm PBS and incubated for 30 minutes with the following antibodies: CD324 (E-cadherin) -Alexa Fluor 647 (BioLegend, CA) and CD325 (N-cadherin)- PerCP-Cy 5.5 (BD Biosciences, NJ). Isotype-matched immunoglobulins, used in same concentrations as that of the primary antibody, served as controls for non-specific immunofluorescence. After incubation cells were analyzed using BD LSRFortessa Cell Analyser flow cytometer and BD FACS-Diva™ v6.2 software.

Statistical analysis

Quantitative RT-PCR and flow cytometry data were analyzed using GraphPad Prism, version 6.0 (GraphPad Software Inc, CA). The means and SEM were calculated for each data set. One-way analysis of variance (ANOVA) with Tukey's multiple comparisons tests and Student's

t test were used for analyzing differences between experimental groups as indicated in the figure legends. A value of $p < 0.05$ was considered significant.

RESULTS

Age-related changes in Foxn1 and Mmp-9 expression in uninjured skin

Analysis of *Foxn1* mRNA expression in skin tissues was performed on enzymatically isolated epidermis collected from young, adult, and old B6 mice (Figure 2A). The similar levels of epidermal Foxn1 expression was detected in young and adult animals and higher levels in old mice (Figure 2A). To explore the localization of Foxn1-eGFP positivity, fluorescent and immunohistochemical detection assays were performed on uninjured skin sections from Foxn1::Egfp mice (Figure 2B and C). Foxn1-eGFP signal localized to the interfollicular epidermis and to hair follicles (Figure 2B). The fluorescent signal of eGFP specificity was confirmed using anti-eGFP immunohistochemical detection assays showing brown reactivity deposits localized to the epidermis and hair follicles (Figure 2C).

Flow cytometric analysis was performed to determine the percentage and phenotype of Foxn1 expressing cells in uninjured skin tissues (Figure 2D–F, Supporting Information Figure 1). Foxn1::Egfp new born, adult, and old mice were used for epidermis collection followed by keratinocyte isolation and subsequent flow cytometric analyses (Figure 2 D–F). The highest percentage of Foxn1-eGFP positive cells was detected in the epidermis of new born mice ($14.8\% \pm 0.6$; Figure 2D and E). Adult and old animals showed $7.2\% \pm 1.5$ and $9.3\% \pm 1.0$ of Foxn1-eGFP positive cells, respectively (Figure 2Dand E).

Within the Foxn1-eGFP positive cell population, phenotypic characterization revealed the highest percentage category as epithelial marker E-cadherin[16] positive cells (Figure 2F, Supporting Information Figure 1). There were no statistically significant differences in the E-cadherin positive cell content between new born ($53.65\% \pm 2.3$), adult ($54.37\% \pm 2.3$), and old ($55.79\% \pm 1.5$) animals (Figure 2F). In contrast, the mesenchymal marker N-cadherin[16] positive cells comprised $0.68\% \pm 0.2$, $0.34\% \pm 0.1$, and $0.4\% \pm 0.1$ for new born, adult, and old mice, respectively. Interestingly, within the Foxn1-eGFP positive cell population, double positive E-cadherin/N-cadherin cells accounted for $23.75\% \pm 1.8$ in new born mice which is more than four and two times more relative to adult and old animal groups, respectively; adult animals showed $5.49\% \pm 1.0$ of E-cadherin/N-cadherin positivity whereas $10.81\% \pm 3.1$ was displayed by old animals (Figure 2F, Supporting Information Figure 1).

Since our published data[12] suggested a possible link between Foxn1 and Mmp-9, we next investigated the expression of *Mmp-9* (Figure 3A). Analysis of enzymatically separated epidermis showed the highest levels of *Mmp-9* expression in the young and old animals (Figure 3A).

Immunofluorescent analysis of uninjured skin tissues from Foxn1-eGFP animals showed Mmp-9 expression in all layers of epidermis and in hair follicles (Figure 3B–D). Colocalization of Foxn1-eGFP and Mmp-9 signals was detected in the suprabasal but not the basal (eGFP-free) layer of epidermis (Figure 3B–D).

Foxn1 expression in postwounded skin tissues in relation to animal age

Generally, levels of *Foxn1* expression change during the course of the skin wound healing process regardless of the animal's age (compare Figure 4A–C). qRT- PCR analysis demonstrated a gradual decrease of *Foxn1* expression from Day 0 (uninjured skin samples) through Days 1, 5 and 7 after injury, followed by its increase at Day 14 and 21 after injury (Figure 4B and C). This pattern of *Foxn1* expression was characteristic for postwounded skin samples of adult (Figure 4B), and old (Figure 4C) mice. Young mice displayed a slightly different profile of *Foxn1* expression (Figure 4A). After the initial decrease at Day 1, a robust increase in *Foxn1* expression was detected at postwounded Days 5, 7, and 14 (Figure 4A). The lowest levels of *Foxn1* expression in postwounded skin samples from young animals were observed at postwounded Days 21 and 36 (Figure 4A).

Flow cytometric analysis of cells isolated from postwounded (Days 7 and 21) skin tissues of adult Foxn1::Egfp mice showed a significant increase in the percentage of eGFP positive cells at postwounded Day 21 (Figure 4D and F; compare: control (uninjured skin; $3.5\% \pm 3.5$), postwounded Day 7 ($2.3\% \pm 0.6$) and postwounded Day 21 ($6.6\% \pm 1.0$).

These data are in agreement with qRT-PCR analysis for adult and old mice showing low (Day 7) and then higher (Day 21) *Foxn1* mRNA expression (see Figure 4B and C). The majority of Foxn1-eGFP cells were E-cadherin positive comprising $57.59\% \pm 6.0$ for uninjured controls, $42.52\% \pm 3.8$ for Day 7 and $65.5\% \pm 4.6$ for Day 21 after injury (Figure 4E, Supporting Information Figure 2). However, the most substantial changes in phenotype of Foxn1-eGFP cells were observed for E-cadherin/N-cadherin double positive cells. Cells isolated at postwounded Day 7 showed an increase in E-cadherin/N-cadherin positive cells ($13.88\% \pm 3.9$) vs. uninjured (3.27 ± 0.9). Cells isolated at postwounded Day 21 displayed $4.55\% \pm 1.7$ of E-cadherin/N-cadherin positive cells (Figure 4E).

Changes in Foxn1 expression during the early (Days 1–7) stage of skin wound healing

Next, we examined Foxn1 localization through eGFP fluorescence and eGFP immunohistological detection in postwounded skin tissues of Foxn1::Egfp mice (Figure 5). At postinjured Day 5, the full thickness wound margins and the fully re-epithelialized epidermis were characterized by evident Foxn1-eGFP expression (Figure 5A and B). Foxn1-eGFP signal was present through all layers of the neo-epidermis except the basal layer (Figure 5C–F). E-cadherin staining was detected throughout the entire epidermis and colocalized with Foxn1-eGFP positive epidermal cells (Figure 5C–F). Interestingly, skin tissues of adult and old animals at postwounded Day 7 showed Foxn1-eGFP positivity not only in neo-epidermis but in the dermal part adjacent to the epidermis (Figure 5G and H).

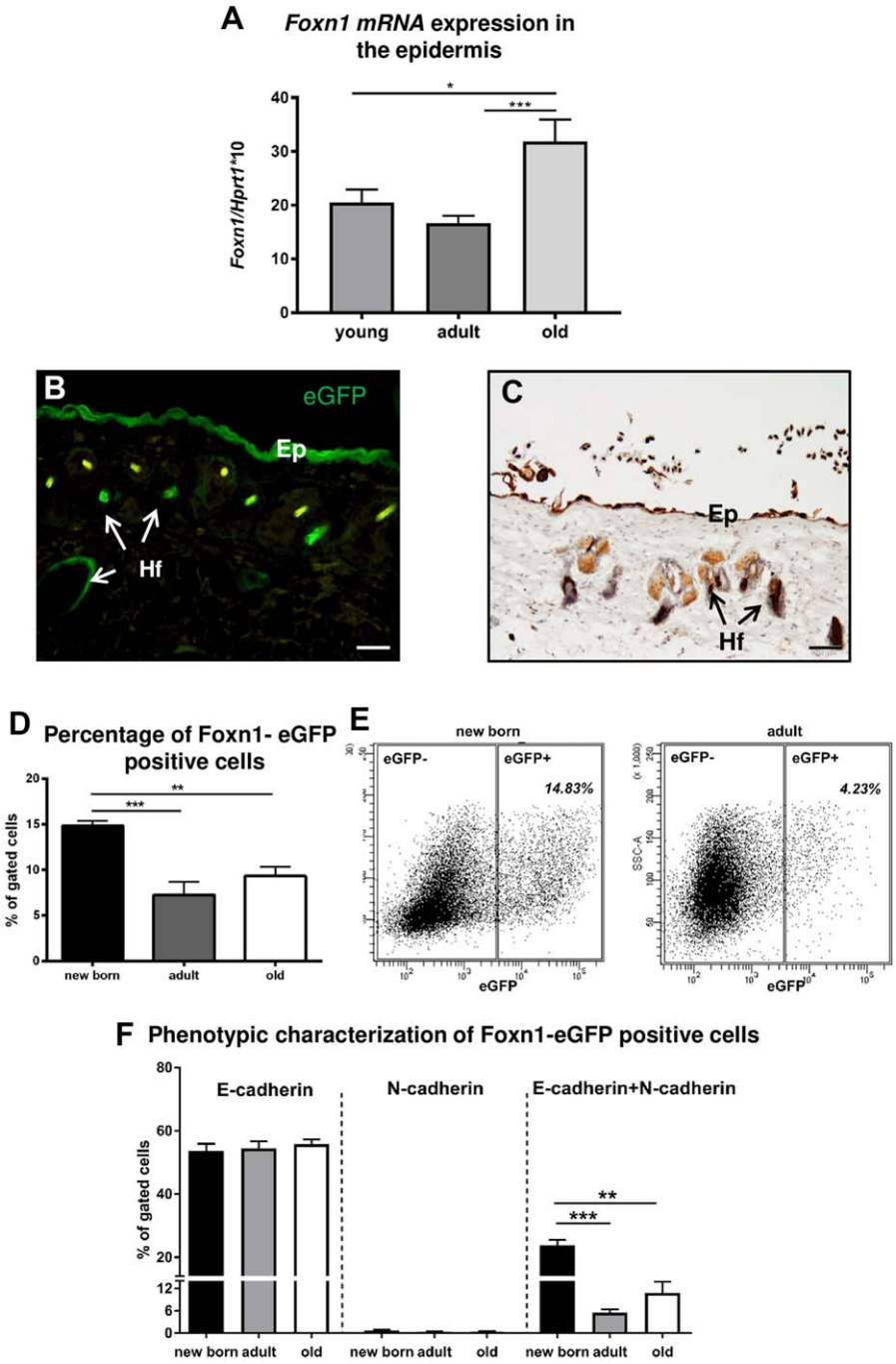

Figure 2. Analysis of Foxn1 expression in uninjured skin tissues from B6 (A) and Foxn1::Egfp (B–F) mice in relation to animal age. qRT-PCR analysis of *Foxn1* mRNA expression in isolated epidermis (A) of young, adult, and old mice. Immunofluorescent (B) and immunohistochemical (C) detection of Foxn1-eGFP signal in skin tissues from adult Foxn1::Egfp mice; scale bar (B) 50 μm, (C) 200 μm. Flow cytometric analysis of keratinocytes isolated from the skin of new born, adult, and old Foxn1::Egfp mice (D–F): percentage of Foxn1-eGFP positive keratinocytes (D, E), percentage of E-cadherin, N-cadherin, and E-cadherin/N-cadherin positive keratinocytes within eGFP+ population (F). Values are the mean ± SEM; $p < 0.05$ (*); $p < 0.01$ (**); $p < 0.001$ (***). [Color figure can be viewed at wileyonlinelibrary.com]

Changes in Foxn1 expression during the late (Days 14–36) stage of skin wound healing

At postwounded Days 14, 21, and 36, a thin epidermis covered the wound area with detectable Foxn1-eGFP expression (Figure 6). The dermal part of the postwounded skin formed two layers: an upper, papillary dermis and a lower, reticular dermis which were clearly distinguishable at postwounded Day 21 (Figure 6A–C). Counterstaining with DAPI showed that the papillary layer consisted of cells with nuclei oriented perpendicular to the epidermis (Figure 6C and D). The papillary dermis was formed by densely packed cells, some of which showed Foxn1-eGFP positivity (Figure 6B–D). Immunofluorescent detection

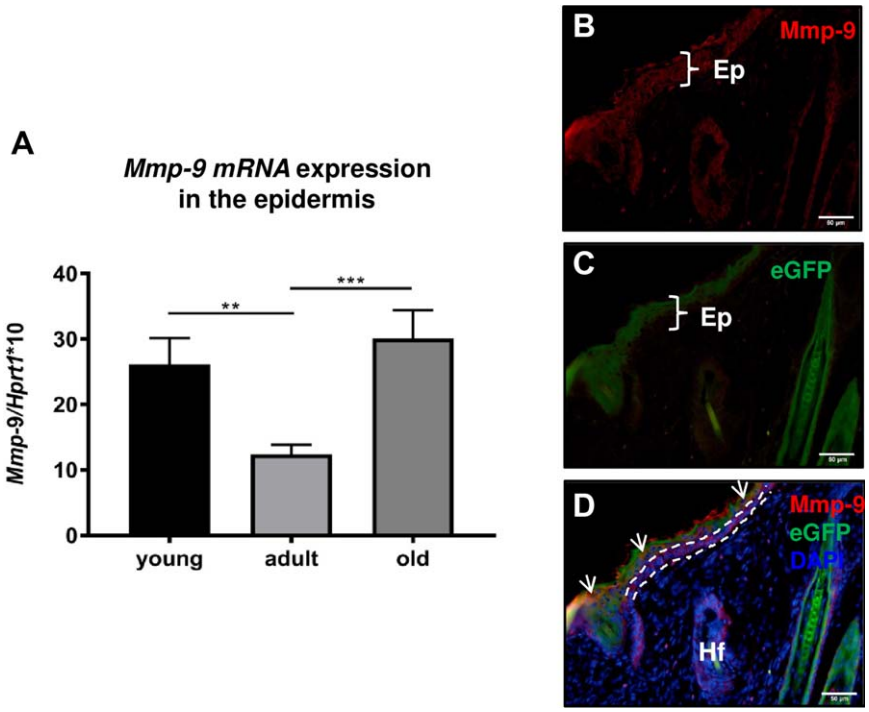

Figure 3. *Mmp-9* mRNA expression in isolated epidermis (A) and Mmp-9 and Foxn1 colocalization (B–D) in uninjured skin from B6 (A) and Foxn1::Egfp (B–D) mice. (A) values are the mean ± SEM; $p < 0.01$ (**); $p < 0.001$ (***). Fluorescent colocalization (D) of Foxn1-eGFP (green); (C) and Mmp-9 (red); (B) in epidermal part of the skin of Foxn1::Egfp mice. Dashed lines delineate epidermal basal layer (D), white arrows indicate colocalization (orange) of Foxn1-eGFP (green) and Mmp-9 (red) positivity. Scale bar 50 μm. [Color figure can be viewed at wileyonlinelibrary.com]

assays showed colocalization of αSMA with some Foxn1-eGFP positive cells present in the papillary dermis (Figure 6B and C). Few Foxn1-eGFP cells in the papillary dermis displayed E-cadherin positivity (Figure 6D). Postwounded skin tissues at Day 36 displayed thin layers of Foxn1-eGFP positive epidermis of equal thickness along the entire length of the healed wound (Figure 6E). However, the newly formed epidermis covering the wound was thinner than the epidermis of uninjured area (Figure 6E).

Changes in Mmp-9 expression in postwounded skin tissues

Mmp-9 plays a key role during skin wound healing process, participating in migratory and remodeling events.[17] The analysis of *Mmp-9* in postwounded skin tissues revealed changes in the mRNA expression levels during the course of the skin wound healing process. We observed a surge in *Mmp-9* expression during postwounded Days 1–5 followed by a gradual decrease between Days 5 and 14 (Figure 7A–C). While an increase in *Mmp-9* expression levels was detected at postwounded Days 21 and 36, this did not achieve statistical significance. Nevertheless, this pattern of *Mmp-9* expression was observed in all groups, regardless of animal age (Figure 7A–C). Immunofluorescent detection of Mmp-9 in postwounded skin samples from Foxn1::Egfp mice showed its localization to the epidermis and to cells dispersed through the dermis (Figure 7D–I). Mmp-9 colocalized with Foxn1-eGFP in the epidermis except in the basal layer, which showed positivity for Mmp-9 but was negative for Foxn1-eGFP expression (Figure 7D–E and G). However, the leading epithelial tongue at postwounded Days 2–4 showed colocalization of Foxn1-eGFP and Mmp-9 through its entire extent and thickness (Figure 7F). Postwounded tissues at Days 14–36 showed a thin layer of epidermis where some Mmp-9 positive cells colocalized with Foxn1-eGFP bearing cells (Figure 7H and I). Papillary dermis at postwounded Day 21 displayed Foxn1-eGFP positive cells, some with colocalized Mmp-9 expression (Figure 7H). Interestingly, postwounded skin tissues at Day 36, collected from old animals did not show two layers of dermis as observed for adult animals (compare Figure 6D and E). Instead, uniformly dispersed Foxn1-eGFP negative cells with few Mmp-9 positive cells repopulated the wound bed (Figure 7I).

DISCUSSION

The present study examined the spatial and temporal expression of Foxn1 and Mmp-9 in the intact and wounded skin as a function of animal age and stages of the wound healing. Our study revealed that *Foxn1* mRNA expression levels were modulated in young, adult, and old mice by the skin wound healing process. Foxn1-eGFP positive cells colocalized with E-cadherin and Mmp-9 during the first stage of wound healing process implying involvement of Foxn1 in the re-epithelialization process. The presence of Foxn1-eGFP and E-cadherin/N-cadherin (epithelial/mesenchymal markers) positive cells together with colocalization of Foxn1-eGFP and myofibroblast marker αSMA cells in papillary dermis at remodeling phase identified the transcription factor Foxn1 as a potential regulator of the skin wound healing process. The present data support and expand our earlier studies performed on young (28- to 35-day old) mice at the early stages (Days 1–7) of skin

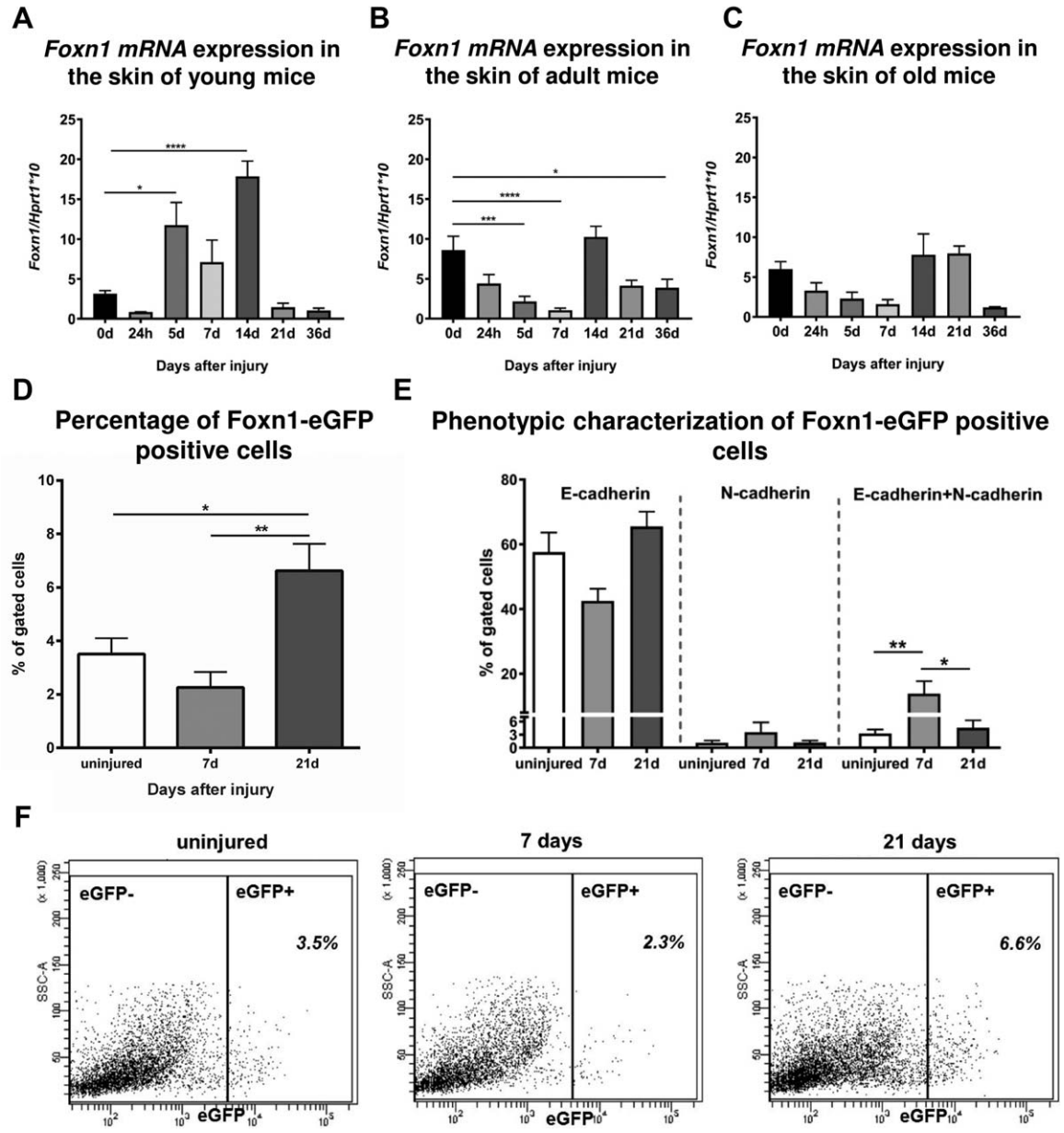

Figure 4. qRT-PCR Foxn1 mRNA expression (A–C) and flow cytometry characterization of Foxn1-eGFP positive cells (D–F) in uninjured and postinjured skin tissues. Skin samples collected from: (A) young, (B) adult, and (C) old B6 mice. Values are the mean ± SEM; $p < 0.05$ (*); $p < 0.01$ (**); $p < 0.001$ (***); $p < 0.0001$ (****); p value calculated from the differences between control (0d/uninjured) and postwounded (Days 1, 5, 7, 14, 21, 36) tissues. Flow cytometry analysis of cells isolated from uninjured ($n = 6$) and postwounded skin tissues of adult Foxn1::Egfp mice at postwounded Day 7th and 21th ($n = 5$–9 per group). Percentage of Foxn1-eGFP positive cells (D and F). Percentage of E-cadherin, N-cadherin, and E-cadherin/N-cadherin positive cells within Foxn1-eGFP+ populations. Data represents mean ± SEM; $p < 0.05$ (*); $p < 0.01$ (**).

wound healing showing Foxn1 engagement in re-epithelialization and in the EMT processes.[12]

Foxn1 expression in uninjured skin of young, adult, and old mice

Foxn1 expression is restricted to epithelial cells, both in the skin and in the thymus.[9,14,18] In the thymus, a comprehensive analysis showed that the progressive decline of Foxn1 expression is associated with age-related degeneration of the thymus.[19,20] Our analysis of skin tissues confirmed Foxn1 localization to epithelial cells, particularly the suprabasal layer of epidermis, and to hair follicles, regardless of the animal's age.[21] However, in contrast to the thymus, measurements of *Foxn1* mRNA

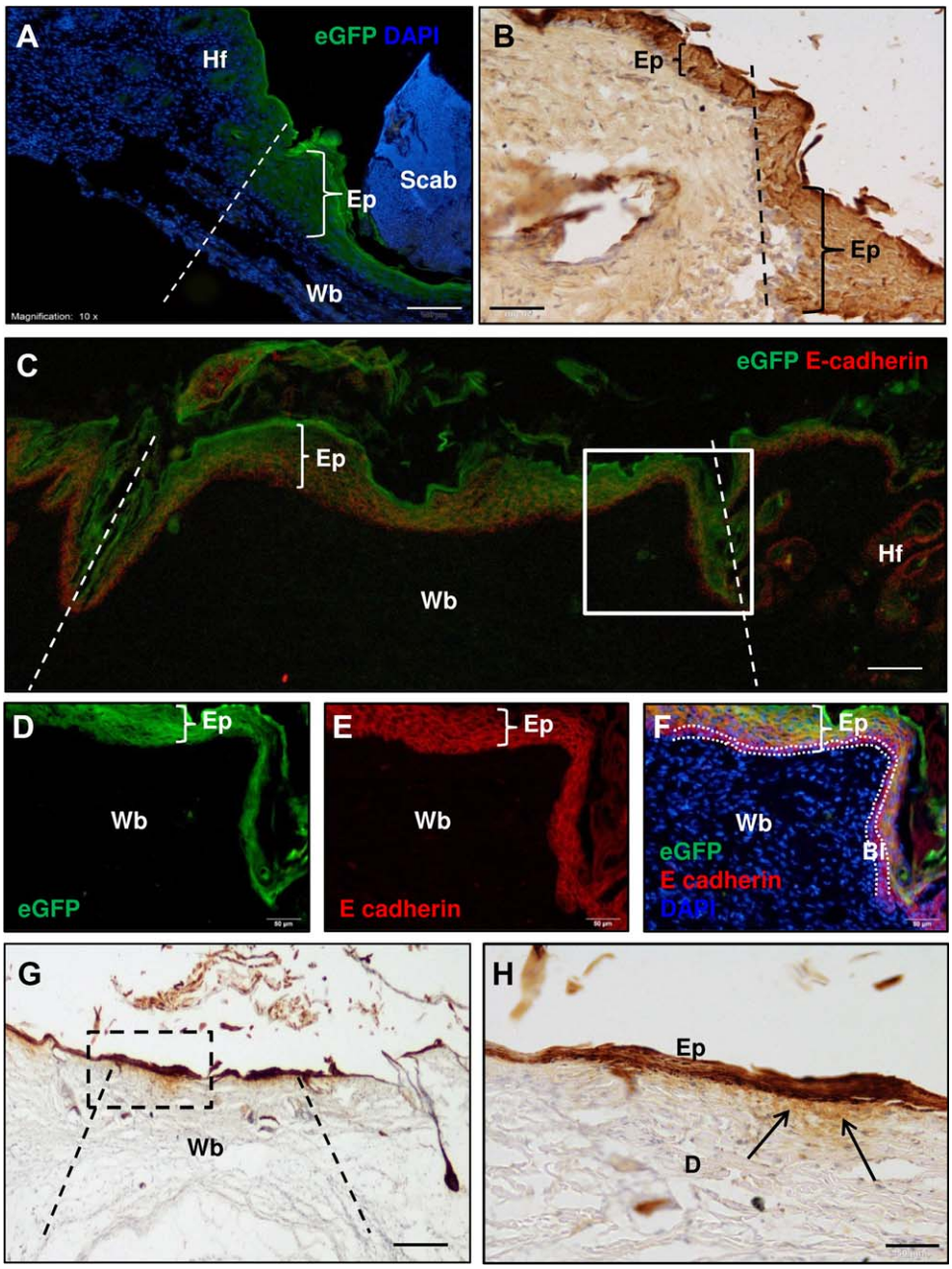

Figure 5. Immunofluorescent (A, C–F) and immunohistochemical (B, G–H), characteristics of skin tissues from Foxn1::Egfp mice at postwounded Days 1–7. Skin tissues collected at Day 5 (A, B) and Day 7 (C–H) after injury from young (C–F), adult (A–B), and old (G–H) animals. Figures (D–F) are a magnification of a box marked at Figure (C); Figure (H) is a magnification of a box marked at Figure (G) Hf - hair follicles, Ep - epidermis, Wb - wound bed, D - dermis, dashed lines indicate wound margins (A, B, C, and G), dotted lines delineate epidermal basal layer (F), black arrows indicate positive immunohistochemical reaction for eGFP positivity in dermis (G H);. Scale bars 50 μm (B, D, E, F, H); 100 μm (A, G,); 200 μm (C). [Color figure can be viewed at wileyonlinelibrary.com]

expression levels by qRT-PCR analysis in uninjured epidermis samples did not show expected decline with animal age. Our study is among the first to investigate Foxn1 expression in mouse skin up to the 18th month of age. Since our study was restricted to qRT-PCR analyses, the lack of Foxn1 protein analysis reflects a potential limitation of the study; however, Western blot analyses performed with commercially available Foxn1 antibodies led to false positive results as described previously.[12] Consequently, we instead used a flow cytometric assay to estimate the percentage of Foxn1-eGFP positive cells and characterized this phenotype as a surrogate for direct Foxn1 protein analyses. Flow cytometric analysis of keratinocytes isolated from the skin of Foxn1::Egfp mice confirmed that *Foxn1* mRNA expression results showed no differences in the percentage of Foxn1-eGFP positive cells between adult and old mice. However, a relatively high percentage of Foxn1-eGFP positive cells was detected in the cell isolates from the epidermis of new born mice. Interestingly, phenotypic characterization of Foxn1-eGFP positive cells from new born mice revealed a large population of E-cadherin/N-cadherin double positive cells.

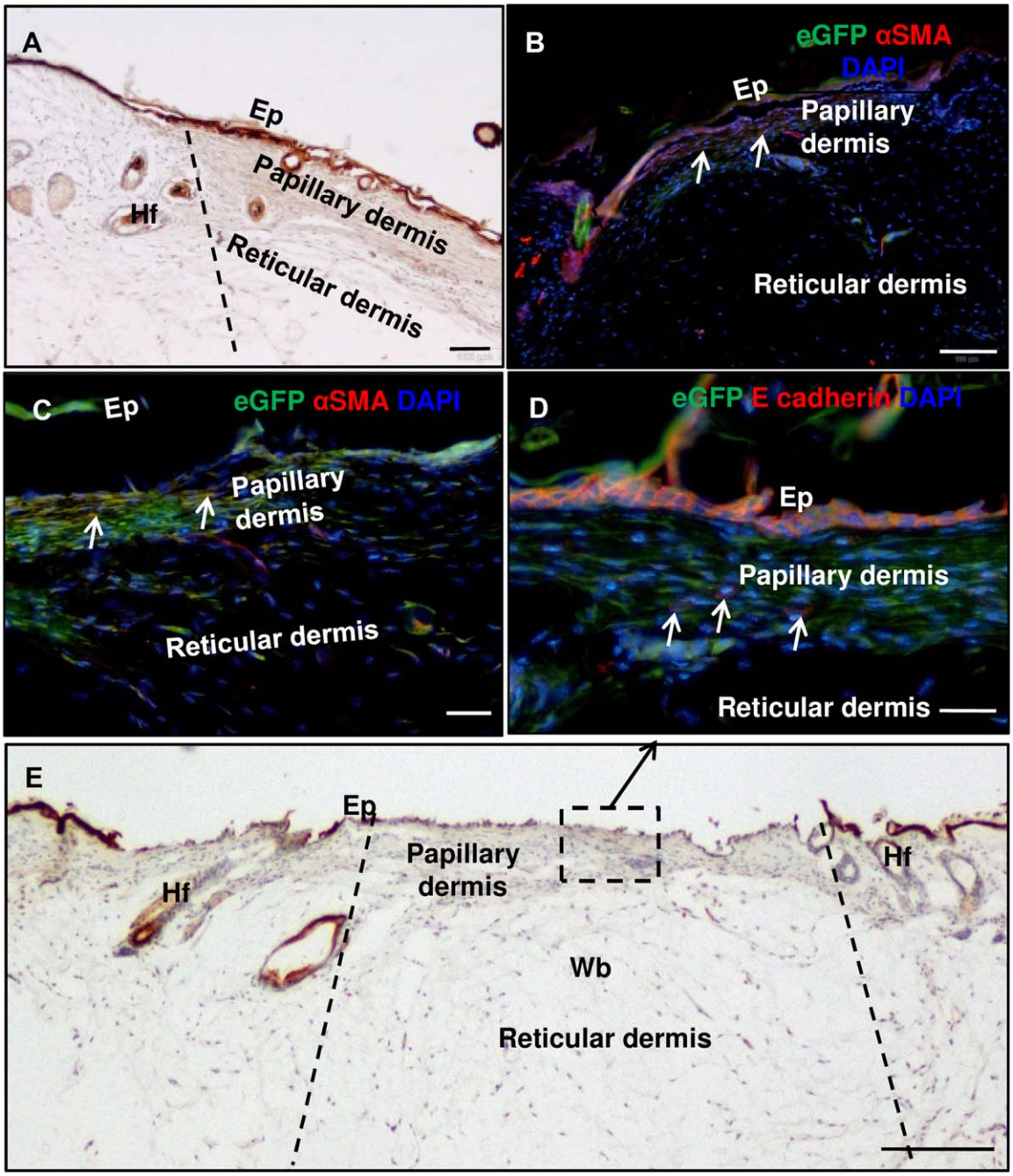

Figure 6. Immunohistochemical (A, E) and immunofluorescent (B–D) characteristics of skin tissues from Foxn1::Egfp mice at postwounded Days 14–36. Skin tissues collected at Day 21 (A–C) and Day 36 after injury (D–E) from adult (A–C) and old (D–E) animals. Figure (D) is a consecutive slide of tissue presented at figure (E). Hf - hair follicles, Wb - wound bed, Ep – epidermis, dotted lines indicate wound margin, white arrows point at: eGFP and αSMA colocalization (B–C), E-cadherin positive cells (D). Scale bars 50μm (D); 100 μm (B); 200 μm (A, E). [Color figure can be viewed at wileyonlinelibrary.com]

Whether the presence of Foxn1/E-cadherin/N-cadherin triple positive cells is indicative of the EMT process, as suggested by Kong et al. in studies of murine skin between embryonic day 18.5 to postnatal Day 9,[22] will require further study.

Foxn1 expression in postwounded skin tissues in relation to animal age

The analysis of postwounded skin tissues showed that during the course of the wound healing process, levels of

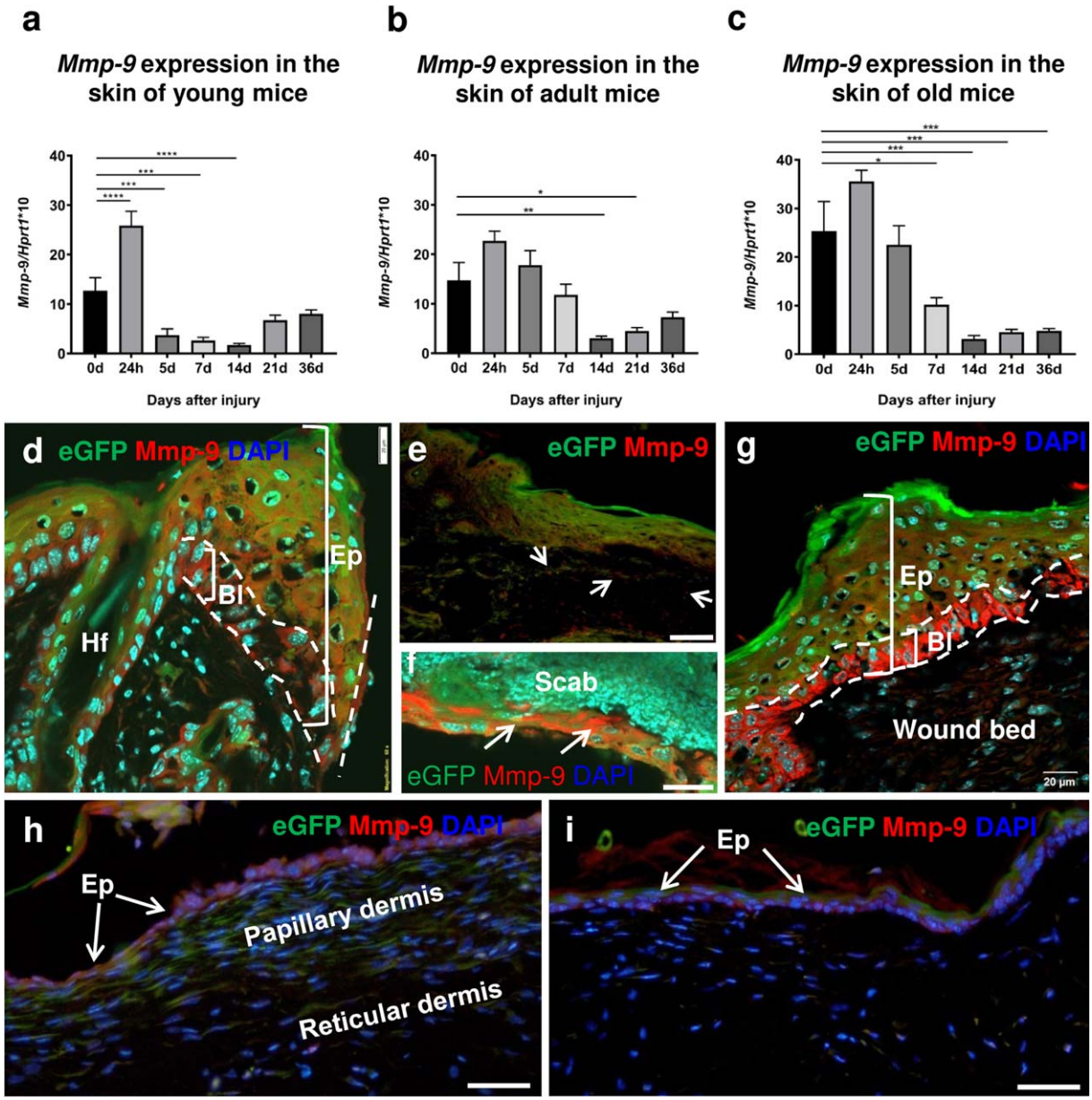

Figure 7. qRT-PCR (A–C) and immunofluorescent (D–I) analysis of Mmp-9 expression in postwounded skin of B6 (A–C) and Foxn1::Egfp (D–I) mice. qRT-PCR analysis of *Mmp-9* expression in young (A), adult (B), and old (C) B6 mice. Values are the mean ± SEM; $p < 0.05$ (*); $p < 0.01$ (**); $p < 0.001$ (***); $p < 0.0001$ (****); p value calculated from the differences between control and postwounded tissues. Immunofluorescent detection of Mmp-9 in skin tissues collected from adult (D–G) and old (H–I) Foxn1:Egfp mice at 2 (D), 3 (E), 4 (f), 6 (G), 21 (H), and 36 days (I) after injury. Ep - epidermis, Bl - basal layer of epidermis, Hf - hair follicles, Wb - wound bed, Wm – wound margin, arrowheads—cells positive for Mmp-9 (E), arrows—leading epithelial tongue (F). Scale bars 20 μm (D, E, F); 50 μm (H, I); 100 μm (E). [Color figure can be viewed at wileyonlinelibrary.com]

Foxn1 gene expression changed, showing profile similarities between adult and old mice. Slightly different profiles of Foxn1 expression were observed in young animals. This discrepancy can be related to the highly synchronized first cycles of hair follicle development during which *Foxn1* plays a crucial role. mRNA expression levels of *Foxn1* in the follicular epithelium declines during the catagen phase (which lasts from Days 16 to 20 after birth) and is very low in telogen phase (from Days 21 to 25–28 after birth).[23,24] The highest *Foxn1* expression in hair follicles has been detected in the anagen phase which begins Days 25–28 after birth and coincides with the age of the youngest animals used in our study. Considering that Days 25–28 after birth are characterized by the highest *Foxn1*

expression in hair follicles,[25] we hypothesize that our observed discrepancy in *Foxn1* expression profile between the young and older age groups can be correlated with the hair growth phase. This intriguing question remains a topic for future investigations.

Our previous studies in which we investigated the changes in Foxn1 expression during the skin wound healing process were performed on young (4- to 5- week old) animals.[12] The study showed that Foxn1 positive cells are involved in the re-epithelialization process during early phase of healing (Days 1–3) and contribute to the EMT process (Days 4–7). We proposed that Foxn1 may participate in scar formation due to its activity in EMT, possibly through Mmp-9 stimulation facilitating epithelial (keratinocytes) to mesenchymal (activated dermal fibroblasts) transition.[12] The present study confirmed and extended our previous analyses. Investigating Foxn1 expression during the remodeling stage of the wound healing process (Days 14–36), we detected Foxn1-eGFP positive cells in the dermal layer of the skin in proximity to the neo-epidermis (papillary dermis). Two distinct lineages of dermal fibroblasts populating the upper, papillary dermis and the lower, reticular dermis were analyzed during age-related skin development and during postwounded skin repair.[26] Driskell et al., demonstrated that epidermal β-catenin activation led to the expansion of the upper, papillary layers by increasing the number of integrin β8 (Itga8+) and Lrig1+ fibroblasts in the wound bed. Consistent with this, our current data shows that Foxn1-eGFP positive cells repopulate the dermal, upper part of postwounded tissues (papillary dermis), displaying the myofibroblast marker αSMA. Using our current observations as a springboard for hypothesis generation, we postulate that the upper, papillary dermis fibroblasts derive in part from a keratinocyte origin. Future studies in our laboratory beyond the scope of the current work will explore the question of whether epidermal β-catenin activation may stimulate Foxn1 positive keratinocytes repopulating the wound neo-epidermis to undergo EMT. We speculate that Foxn1-positivity, together with modulated by Foxn1 signaling pathways via secreted factors that impact dermal fibroblasts, stimulate reparative (scar- forming) skin healing. Our novel data provide evidence for the Foxn1 transcription factor's participation in both the proliferative and remodeling stages of skin wound healing process. Although the mechanism of Foxn1 action will require further investigation, the studies strongly support its role in skin injury repair.

Well documented data of the age related decrease in Foxn1 expression in the thymus epithelium, which correlates with thymus involution,[19,20] spurred our study toward possible age-related changes in skin Foxn1 expression. However, neither gene expression data nor flow cytometric analysis of Foxn1-eGFP positive cells detected an age related decrease in Foxn1 expression in intact skin or differences in Foxn1 modulation during the skin wound healing process in adult vs. old animals. Nevertheless histological analysis showed the temporary and spatial differences in Foxn1-eGFP expressing cells in postwounded skin. In old animals, Foxn1-eGFP signal was detected in the dermis one week earlier than in other groups of mice (14 days comparing to 21 after wounding) and was undetectable at Day 36. This may account for the age-dependent changes occurring in the skin wound healing in aged mice.[27] Further examination will be required to evaluate the role of Foxn1 in skin wound healing process in aged animals.

Age-related changes in Mmp-9 expression in uninjured and in postwounded skin tissues

Another interesting aspect of the present study is the Mmp-9 expression and localization in skin tissue. Foxn1 and Mmp-9 expression in uninjured epidermis and their colocalization during the re-epithelization process suggest that a molecular pathway links Foxn1 and Mmp-9.

In fact, the analysis of skin Mmp-9 expression showed substantial differences between Foxn1 deficient (nude) and wild type mice.[11,28] Uninjured skin of nude displayed higher than wild type mice levels of Mmp-9 expression.[11] This difference has been attributed to nude dermal fibroblasts which express much higher levels of Mmp-9 than B6 mice.[11,28] Moreover, next-generation high-throughput DNA sequencing analysis revealed up-regulation of *Mmp-9* expression in the total skin samples from nude (Foxn1 deficient) mice but down-regulation in enzymatically separated epidermis (unpublished data). Further differences between Foxn1 deficient (nude) and wild type mice were revealed analyzing Mmp-9 expression profile during skin wound healing process.[11] Although skin injury evoked up-regulation of Mmp-9 expression (postwounded Days 1–3) in both mouse strains, the magnitude of up-regulation was much lower in Foxn1 deficient animals. Also, nude mice showed a second surge of Mmp-9 during the late, remodeling phase of wound healing (postwounded Days 21–36). It has been suggested that second weave of Mmp-9 induction can be associated with the ability for scarless healing in nude mice.[11]

Although beyond the scope of the current study, our laboratory will pursue the novel concept that Foxn1 may regulate Mmp-9 expression in the healing epithelium.

In conclusion, the transcription factor Foxn1 participates in the skin wound healing process through engagement in the re-epithelialization process in the early proliferative phase, and in the late, remodeling phase of wound healing. Further studies will be required to identify the mechanisms of Foxn1 action in cutaneous healing which may shed light on treatment approaches to re-direct the wound healing process from one of scar formation toward regeneration.

ACKNOWLEDGMENTS

We thank Professor Thomas Boehm (Max Planck Institute of Immunobiology and Epigenetics, Germany) for generously providing Foxn1::Egfp transgenic mice.

Source of Funding: This study was supported by the National Science Centre Poland Grant OPUS No. DEC-2012/05/B/NZ5/01537. The article processing charge was covered by the KNOW Consortium: "Healthy Animal - Safe Food" (Ministry of Sciences and Higher Education; Dec: 05-1/KNOW2/2015).

Conflict of Interest: Dr. Gimble is the cofounder, co-owner, and Chief Scientific Officer of LaCell LLC. All other authors have no conflict of interest to declare.

REFERENCES

1. Clark RA, Ashcroft GS, Spencer MJ, Larjava H, Ferguson MW. Re-epithelialization of normal human excisional wounds is associated with a switch from alpha v beta 5 to alpha v beta 6 integrins. *Br J Dermatol* 1996; 135: 46–51.
2. Singer AJ, Clark RA. Cutaneous wound healing. *N Engl J Med* 1999; 341: 738–46.
3. Gurtner GC, Werner S, Barrandon Y, Longaker MT. Wound repair and regeneration. *Nature* 2008; 453: 314–21.
4. Rowlatt U. Intrauterine wound healing in a 20 week human fetus. *Virchows Arch A Pathol Anat Histol* 1979; 381: 353–61.
5. Colwell AS, Longaker MT, Lorenz HP. Mammalian fetal organ regeneration. *Adv Biochem Eng Biotechnol* 2005; 93: 83–100.
6. Cass DL, Bullard KM, Sylvester KG, Yang EY, Longaker MT, Adzick NS. Wound size and gestational age modulate scar formation in fetal wound repair. *J Pediatr Surg* 1997; 32: 411–5.
7. Schafer M, Werner S. Transcriptional control of wound repair. *Annu Rev Cell Dev Biol* 2007; 23: 69–92.
8. Bellavia G, Fasanaro P, Melchionna R, Capogrossi MC, Napolitano M. Transcriptional control of skin reepithelialization. *J Dermatol Sci* 2014; 73: 3–9.
9. Mecklenburg L, Tychsen B, Paus R. Learning from nudity: lessons from the nude phenotype. *Exp Dermatol* 2005; 14: 797–810.
10. Gawronska-Kozak B, Bogacki M, Rim JS, Monroe WT, Manuel JA. Scarless skin repair in immunodeficient mice. *Wound Repair Regen* 2006; 14: 265–76.
11. Gawronska-Kozak B. Scarless skin wound healing in FOXN1 deficient (nude) mice is associated with distinctive matrix metalloproteinase expression. *Matrix Biol* 2011; 30: 290–300.
12. Gawronska-Kozak B, Grabowska A, Kur-Piotrowska A, Kopcewicz M. Foxn1 transcription factor regulates wound healing of skin through promoting epithelial-mesenchymal transition. *PLoS One* 2016; 11: e0150635.
13. Terszowski G, Muller SM, Bleul CC, Blum C, Schirmbeck R, Reimann J, et al. Evidence for a functional second thymus in mice. *Science* 2006; 312: 284–7.
14. Calderon L, Boehm T. Synergistic, context-dependent, and hierarchical functions of epithelial components in thymic microenvironments. *Cell* 2012; 149: 159–72.
15. Turabelidze A, Guo S, DiPietro LA. Importance of housekeeping gene selection for accurate reverse transcription-quantitative polymerase chain reaction in a wound healing model. *Wound Repair Regen* 2010; 18: 460–6.
16. Kumarswamy R, Mudduluru G, Ceppi P, Muppala S, Kozlowski M, Niklinski J, et al. MicroRNA-30a inhibits epithelial-to-mesenchymal transition by targeting Snai1 and is downregulated in non-small cell lung cancer. *Int J Cancer* 2012; 130: 2044–53.
17. Clark R. *The molecular and cellular biology of wound repair*. New York: Plenum Press, 1996.
18. Prowse DM, Lee D, Weiner L, Jiang N, Magro CM, Baden HP, et al. Ectopic expression of the nude gene induces hyperproliferation and defects in differentiation: implications for the self-renewal of cutaneous epithelia. *Dev Biol* 1999; 212: 54–67.
19. Bredenkamp N, Nowell CS, Blackburn CC. Regeneration of the aged thymus by a single transcription factor. *Development* 2014; 141: 1627–37.
20. O'Neill KE, Bredenkamp N, Tischner C, Vaidya HJ, Stenhouse FH, Peddie CD, et al. Foxn1 is dynamically regulated in thymic epithelial cells during embryogenesis and at the onset of thymic involution. *PLoS One* 2016; 11: e0151666.
21. Lee D, Prowse DM, Brissette JL. Association between mouse nude gene expression and the initiation of epithelial terminal differentiation. *Dev Biol* 1999; 208: 362–74.
22. Kong W, Li S, Liu C, Bari AS, Longaker MT, Lorenz HP. Epithelial-mesenchymal transition occurs after epidermal development in mouse skin. *Exp Cell Res* 2006; 312: 3959–68.
23. Meier N, Dear TN, Boehm T. Whn and mHa3 are components of the genetic hierarchy controlling hair follicle differentiation. *Mech Dev* 1999; 89: 215–21.
24. Muller-Rover S, Handjiski B, van der Veen C, Eichmuller S, Foitzik K, McKay IA, et al. A comprehensive guide for the accurate classification of murine hair follicles in distinct hair cycle stages. *J Invest Dermatol* 2001; 117: 3–15.
25. Lin KK, Chudova D, Hatfield GW, Smyth P, Andersen B. Identification of hair cycle-associated genes from time-course gene expression profile data by using replicate variance. *Proc Natl Acad Sci USA* 2004; 101: 15955–60.
26. Driskell RR, Lichtenberger BM, Hoste E, Kretzschmar K, Simons BD, Charalambous M, et al. Distinct fibroblast lineages determine dermal architecture in skin development and repair. *Nature* 2013; 504: 277–81.
27. Swift ME, Kleinman HK, DiPietro LA. Impaired wound repair and delayed angiogenesis in aged mice. *Lab Invest* 1999; 79: 1479–87.
28. Gawronska-Kozak B, Kirk-Ballard H. Cyclosporin A reduces matrix metalloproteinases and collagen expression in dermal fibroblasts from regenerative FOXN1 deficient (nude) mice. *Fibrogenesis Tissue Repair* 2013; 6: 7.

SUPPORTING INFORMATION

Additional supporting information may be found in the online version of this article at the publisher's web-site